

Millimetre observations of infrared carbon stars^{*,**}

I. The data

M. A. T. Groenewegen¹, M. Sevenster², H. W. W. Spoon³, and I. Pérez^{2,4}

¹ Instituut voor Sterrenkunde, PACS-ICC, Celestijnenlaan 200B, 3001 Heverlee, Belgium

² Mount Stromlo and Siding Spring Observatory, Cotter road, Weston ACT, Australia

³ Kapteyn Astronomical Institute, Postbus 800, 9700 AV, Groningen, The Netherlands

⁴ Departamento de Astronomía, Universidad de Chile, Casilla 36-D, Santiago, Chile

Received 1 March 2002 / Accepted 15 May 2002

Abstract. Millimetre observations of IRAS selected red carbon stars are presented. About 260 stars have been observed with SEST and IRAM in the CO (1–0) and CO (2–1) lines and partially in HCN (1–0) and SiO (3–2). An overall detection rate, in at least one line, of about 80% is achieved. The survey represents the second largest survey for AGB stars, and the largest ever for carbon stars. Two new detections in SiO (3–2) in carbon stars are reported. When available, the SiO/HCN and HCN/CO (1–0) line ratios are consistent with the ratios expected for carbon stars.

Key words. circumstellar matter – stars: mass-loss – stars: AGB and post-AGB

1. Introduction

The orbits of stars, moving in the global potential of the Galaxy, are functions of the integrals of motion in that potential only. For an axisymmetric potential, under the assumption that the radial-velocity dispersion equals the vertical-velocity dispersion, these integrals are the binding energy E and the vertical angular momentum L_z . The dynamical behaviour of a particular sample of stars is then fully characterised by a distribution function in these two variables (see Sevenster et al. 1995, and references therein). This distribution function is found by comparing the moments of the observed distribution to the projected moments of model distributions on a grid in galactic coordinates l, b . The noise in the input moments is, naturally, dependent of the number of stars observed, and typically a few hundred stars are necessary to constrain models on an extended region of the sky. The comparison is performed with a quadratic-programming method (DeJonghe 1989). The spatial

distribution and the kinematics of a certain population of stars will in general not be self-consistent, since the velocities are determined by the global potential rather than the potential derived from the spatial distribution via Poisson's equation. This is fully taken into account by the modelling method. The resulting analytic distribution functions can very easily be used for further analysis. For Galaxy studies, the technique has been successfully applied to Planetary Nebulae (Durand et al. 1996) and OH/IR stars (Sevenster et al. 1995).

Some time ago, we started a study into the dynamical behaviour of carbon stars. The aim of this project is to compare the dynamical behaviour of carbon stars to OH/IR stars and to test the hypothesis that the so-called “infra-red” carbon stars form a more massive population than the traditional well-known “optical” carbon stars (see e.g. Groenewegen et al. 1995). To investigate this, we acquired two samples. One sample of 700 optical carbon stars, for which radial velocities are available, was taken from Aaronson et al. (1989, 1990). The analysis was done on a smaller sub-sample of 500 that was selected to make the sample more homogeneous. First results are presented in Sevenster et al. (2000). As expected for such relatively low-mass AGB stars the scale height is large (650 vs. 200 pc for low-latitude OH/IR stars). There is no discontinuity between their dynamical distribution and that of the low-mass OH/IR stars, showing that, despite the very different radial ranges occupied by O-rich and C-rich stars, these do form one dynamical (AGB) population.

To ascertain that this applies to all AGB stars, a second sample of infrared carbon stars, to be compared to the more

Send offprint requests to: M. Groenewegen,
e-mail: groen@ster.kuleuven.ac.be

* Based on observations collected at the European Southern Observatory, La Silla, Chile within program ESO 60.E-0103, 62.L-0128, 64.L-0012 and 66.D-0027. Also based on observations with the IRAM telescope, Granada, Spain under programs 98-97, 141-97 and 010-99

** The complete Fig. 1 is only available in electronic form at <http://www.edpsciences.org>. The complete Table 3 is only available in electronic form at the CDS via anonymous ftp to cdsarc.u-strasbg.fr (130.79.128.5) or via <http://cdsweb.u-strasbg.fr/cgi-bin/qcat?J/A+A/390/501>

massive OH/IR stars, was selected from the literature, as discussed below. Since only part of those have known radial velocities, an observational program was initiated to obtain radial velocities for the other stars. As these stars, almost by definition, have weak or no optical counterparts and thick circumstellar shells, the most efficient way to obtain the radial velocity is through millimetre line spectroscopy.

The main aim of the paper is therefore to provide the radial velocities of a large sample of infrared carbon stars as input to further analysis of the dynamical properties of carbon stars. However, as a by-product, the expansion velocities and line strengths are also obtained of the stars. The sample is introduced in Sect. 2, and the observations are presented in Sect. 3. The results are briefly discussed in Sect. 4.

The new observations are combined with mm-data available in the literature and analysed in terms of the spatial dependence of the expansion velocity, dust and gas mass loss rate and replenishment of the interstellar medium in the accompanying paper (Groenewegen et al. 2002). The analysis of distribution functions and the comparison to the dynamical properties of other populations of evolved stars will be reported in a third paper (Sevenster et al. 2002, in preparation).

2. The sample

The sample of (very probable) infrared carbon stars was selected as follows. In a first step, objects that fulfilled the following criteria were selected from the IRAS Point Source Catalog version 2 (PSC): Flux quality 3 at 12 and 25 μm , and ≥ 2 at 60 μm , flux ratios $S_{12}/S_{25} < 3$, $S_{25}/S_{60} > 2.75$, and finally $S_{12} > 20 \text{ Jy}$ or IRAS LRS classification equal to 4n. The former flux-ratio is used to select stars with an far-IR excess, while the latter flux-ratio assures that red OH/IR stars and Planetary Nebulae are excluded. Applying these criteria resulted in 2088 stars which contains M- and S-stars as well.

In the next step, the following stars were removed: those which are associated in the PSC with the catalogue of S-stars, and stars with a spectral type M in the Michigan or SAO catalogue (as listed in the PSC).

In the next step, the IRAS LRS spectra (from the LRS catalogue, Volk & Cohen 1989, Volk et al. 1991) and the SIMBAD database were checked for the remaining stars. A detection in a SiO or OH thermal or maser line implied that the star would not be observed by us. The visual inspection of the LRS spectra ensured that stars with silicate emission, but nevertheless classified as 4n, were removed.

There are known infrared carbon stars which are not classified as LRS = 4n, namely the extremely red carbon stars (Group v in Groenewegen et al. 1992; also see Volk et al. 1992). From these papers we selected those stars that fulfilled the same criteria on flux-quality and flux ratios as above.

The total sample contains 379 stars. For those we searched in the literature (up to January 1997 when this program was originally initiated) for available radial velocities from CO line emission. Hundred twenty-four stars have a reliable radial velocity reported (from the Loup et al. 1993 catalogue, Kastner et al. 1993 and Groenewegen et al. 1996; also see

Neri et al. 1998, Knapp et al. 1998, Josselin et al. 1998 for improved observations for a few of these stars). The remaining 255 were put on the observing list and here we report on millimetre observations of these stars.

3. The observations

Observations were performed with IRAM on 3 different occasions and with the SEST on 4 different occasions. The stars that were observed during the different runs are listed in Table 1; some stars were observed more than one time. Table 1 also lists the coordinates used in the observations which have been taken from the IRAS database. The accuracy of these coordinates is of order 10–15'' which is comparable to the smallest beam size used here (CO 2–1 beam at IRAM). However the detection rate at IRAM is 90%, and of the non-detections 5% are likely inhibited by interstellar contamination so that non-detections due to incorrect input coordinates are a minor issue.

The IRAM data were taken between 18 and 22 October 1997 (observers MG and HS), 22 and 28 April 1998 (observer MG) and between 23 and 27 July 1999 (observers MG and MS). In October 1997 the ^{12}CO (2–1), HCN (1–0) and SiO (3–2) lines were observed simultaneously using the 1.3 mm, 2 mm and 3 mm SIS receivers. Detection of the HCN or SiO line could confirm or deny the carbon star character. Both the two 1 MHz filter banks (for CO and SiO) and the auto correlator (for HCN, set to a channel spacing of 320 KHz) were used as back-ends.

In April 1998 the same configuration of front-ends, back-ends and observed lines was used for the first four observing slots. For the final two slots both 3 mm receivers were tuned to the ^{12}CO (1–0) lines, and both 1.3 mm receivers were tuned to the ^{12}CO (2–1) line. The 1 MHz back-end was split and connected to the 1.3 mm receivers, and the auto correlator was split and connected to the 3 mm receivers (channel spacing 320 kHz). The brightest sources had preferentially been observed first and based on the results, it seemed unlikely to detect HCN in the weaker sources. On the other hand, with the new set-up a theoretical gain of $\sqrt{2}$ in signal-to-noise could be obtained on the CO lines, which turned out to be useful as many of our detections are quite faint.

In July 1999, HCN, ^{12}CO (1–0) and ^{12}CO (2–1) were observed simultaneously. The 1 MHz back-end was used on the CO (2–1) line, and the auto correlator was set to a channel spacing of 320 KHz and used for CO (1–0) and HCN.

On all occasions the targets were observed using wobbler switching with throws between 90 and 150'' in azimuth; pointing and focus were checked every few hours.

The SEST data were taken between 10–12 and 14 March 1998 (observer MG), 9 and 14 March 1999 (observer MG), 23 and 28 October 1999 (observer MG), and between 25 and 31 March 2001 (observers MG and IP). On all occasions, ^{12}CO (1–0) and ^{12}CO (2–1) were observed simultaneously using the 1.3 mm and 3 mm SIS receivers. The dual beam switching mode was used with a throw of 2'26'' in azimuth. One of two available acousto-optical spectrometers was split and connected to the two receivers. The channel separation is 0.7 MHz. Focus and pointing were checked every few hours, and almost

Table 1. The stars observed.

IRAS Name	RA (1950)	Dec (1950)	Observed
00422+5310	0 42 16.7	53 10 24	iram jul99
01022+6542	1 02 12.6	65 42 54	iram apr98
01080+5327	1 08 02.3	53 27 38	iram apr98
01443+6417	1 44 19.6	64 17 58	iram apr98
02345+5422	2 34 34.6	54 22 19	iram apr98
02596+6639	2 59 37.5	66 39 30	iram jul99
03157+3258	3 15 42.9	32 58 40	iram apr98; sest mar01
03238+6034	3 23 52.3	60 34 30	iram apr98
03277+5120	3 27 44.5	51 20 09	iram jul99
03293+6038	3 29 21.6	60 38 20	iram apr98
03385+5927	3 38 34.1	59 27 30	iram apr98
03557+4404	3 55 42.1	44 04 39	iram apr98
04127+5030	4 12 45.9	50 30 09	iram jul99
04179+5951	4 17 55.6	59 51 43	iram apr98
04297+2941	4 29 45.2	29 41 49	iram apr98; iram jul99; sest mar01
04365+6349	4 36 31.3	63 49 11	iram oct97
04369+4501	4 36 55.0	45 01 44	iram oct97; iram jul99
04449+4951	4 44 55.7	49 51 53	iram jul99
05223+4704	5 22 23.6	47 04 55	iram oct97; iram apr98
05261+4626	5 26 09.1	46 26 33	iram oct97; iram jul99
05316+1757	5 31 40.1	17 57 56	iram jul99
05428+1215	5 42 48.2	12 15 06	iram jul99
05440+4311	5 44 01.7	43 11 49	iram jul99
05447+1321	5 44 46.6	13 21 36	iram apr98; iram jul99; sest mar01
06003+4747	6 00 21.7	47 47 52	iram oct97; iram jul99
06088+1909	6 08 50.9	19 09 04	iram jul99
06181+0406	6 18 07.3	04 06 36	iram jul99
06183+1135	6 18 19.3	11 35 42	iram jul99; sest oct99
06192+0722	6 19 15.7	07 22 30	iram jul99; sest mar01
06315+1606	6 31 30.9	16 06 55	iram jul99
06323+3015	6 32 19.1	30 15 14	iram jul99; sest oct99
06344-0124	6 34 29.3	-01 24 26	iram jul99
06348+3114	6 34 50.9	31 14 23	iram jul99; sest mar01
06378-0527	6 37 51.3	-05 27 11	sest mar98
06447+0817	6 44 42.5	08 17 18	iram jul99
06462-4157	6 46 16.7	-41 57 44	sest mar99
06471+0301	6 47 08.3	03 01 43	iram jul99
06528-4218	6 52 52.2	-42 18 02	sest mar98
06558+2853	6 55 52.2	28 53 02	iram oct97; sest mar01
06585-4111	6 58 34.4	-41 11 40	sest oct99
06588-2138	6 58 48.3	-21 38 46	iram jul99; sest mar99; sest mar01
07073-1944	7 07 21.9	-19 44 45	sest mar99
07080-0106	7 08 02.5	-01 06 27	iram jul99
07085-0018	7 08 33.7	-00 18 12	sest oct99
07149-0046	7 14 59.5	-00 46 26	sest oct99
07161-0111	7 16 06.2	-01 11 19	iram jul99
07170+0721	7 17 03.9	07 21 32	iram jul99
07220-2324	7 22 01.0	-23 24 50	iram jul99; sest mar99; sest oct99; sest mar01
07266-0541	7 26 41.2	-05 41 21	sest mar99
07336-1006	7 33 40.2	-10 06 10	sest mar98
07356-3549	7 35 37.6	-35 49 20	sest mar99; sest oct99
07368-2833	7 36 50.3	-28 33 41	sest mar98
07373-4021	7 37 22.1	-40 21 49	sest oct99
07546-2551	7 54 37.1	-25 51 41	iram jul99; sest oct99; sest mar01
07553-0907	7 55 27.3	-09 07 51	iram jul99; sest mar01
08086-3905	8 08 39.3	-39 05 20	sest mar98

Table 1. continued.

Name	RA (1950)	Dec (1950)	Observed
08119–3627	8 11 55.7	–36 27 47	sest oct99
08129–1236	8 12 58.0	–12 36 07	iram jul99; sest mar99; sest oct99
08250–2605	8 25 05.8	–26 05 38	sest oct99
08276–5125	8 27 41.9	–51 25 09	sest mar98
08292–3828	8 29 14.4	–38 28 01	sest oct99; sest mar01
08304–4313	8 30 27.7	–43 13 29	sest mar98; sest mar99; sest mar01
08305–3314	8 30 33.9	–33 14 58	sest mar98
08340–3357	8 34 04.3	–33 57 08	sest mar99
08353–3424	8 35 23.3	–34 24 11	sest oct99
08416–2525	8 41 40.4	–25 25 48	sest mar98
08439–2734	8 43 58.1	–27 34 47	sest oct99
08470–5710	8 47 05.6	–57 10 20	sest oct99
08534–5055	8 53 27.2	–50 55 47	sest mar99; sest oct99
08535–4724	8 53 30.4	–47 24 26	sest oct99; sest mar01
08544–4431	8 54 29.5	–44 31 44	sest oct99; sest mar01
08556–5717	8 55 41.3	–57 17 09	sest oct99
09164–5349	9 16 27.6	–53 49 44	sest oct99; sest mar01
09176–5147	9 17 38.5	–51 47 42	sest oct99
09178–5556	9 17 51.9	–55 56 13	sest mar01
09238–5309	9 23 49.5	–53 09 38	sest oct99; sest mar01
09317–5116	9 31 43.0	–51 16 53	sest mar99
09428–4341	9 42 50.8	–43 41 51	sest oct99; sest mar01
09450–4716	9 45 02.0	–47 16 44	sest mar99
09485–4232	9 48 35.2	–42 32 48	sest oct99; sest mar01
09496–5050	9 49 38.1	–50 50 12	sest mar98; sest oct99
09533–6021	9 53 20.3	–60 21 10	sest oct99
09547–5522	9 54 47.7	–55 22 54	sest oct99; sest mar01
09587–5056	9 58 47.6	–50 56 59	sest mar01
10002–4641	10 00 13.0	–46 41 47	sest mar01
10068–6341	10 06 49.0	–63 41 20	sest mar01
10098–5742	10 09 49.5	–57 42 55	sest mar98; sest mar99
10231–5823	10 23 08.4	–58 23 54	sest oct99; sest mar01
10249–2517	10 24 56.5	–25 17 38	sest mar01
10375–4802	10 37 33.2	–48 02 10	sest oct99
10558–6537	10 55 49.3	–65 37 19	sest oct99; sest mar01
11073–6325	11 07 19.2	–63 25 07	sest oct99
11079–6211	11 07 58.3	–62 11 33	sest oct99; sest mar01
11186–5528	11 18 37.4	–55 28 09	sest mar98
11272–6901	11 27 16.9	–69 01 38	sest mar01
11463–6320	11 46 22.0	–63 20 47	sest mar98
11514–5841	11 51 24.6	–58 41 44	sest mar98
12042–6355	12 04 13.0	–63 55 45	sest mar99; sest oct99
12142–6410	12 14 15.6	–64 10 29	sest mar01
12194–6007	12 19 26.2	–60 07 38	sest mar99; sest oct99
12195–6830	12 19 30.8	–68 30 45	sest mar98; sest oct99
12195–5527	12 19 35.4	–55 27 23	sest mar99; sest mar01
12216–6118	12 21 37.1	–62 18 12	sest mar99 (observed at incorrect position); sest mar01
12227–5045	12 22 42.3	–50 45 42	sest mar99
12298–5754	12 29 52.6	–57 54 57	sest mar98
12397–6447	12 39 47.5	–64 47 13	sest mar98; sest oct99
12419–6058	12 41 55.3	–60 58 40	sest oct99
12421–6217	12 42 08.4	–62 17 10	sest mar01
12464–6433	12 46 29.9	–64 33 39	sest mar01
12533–6118	12 53 23.4	–61 18 25	sest mar01
12550–7407	12 55 01.7	–74 07 30	sest mar99
12562–6003	12 56 13.3	–60 03 13	sest mar01
12569–6105	12 56 59.6	–61 05 09	sest mar01
12595–6035	12 59 31.9	–60 35 45	sest mar98; sest mar01

Table 1. continued.

Name	RA (1950)	Dec (1950)	Observed
13031–5743	13 03 08.0	–57 43 18	sest mar01
13045–6404	13 04 33.4	–64 04 21	sest mar99
13053–6341	13 05 18.2	–63 41 37	sest mar98; sest mar99
13064–6433	13 06 25.5	–64 33 56	sest mar99; sest oct99; sest mar01
13092–6026	13 09 16.3	–60 26 56	sest mar01
13208–6027	13 20 52.3	–60 27 49	sest mar01
13268–6226	13 26 51.7	–62 26 22	sest mar98; sest mar99
13343–5613	13 34 21.7	–56 13 21	sest mar01
13343–5807	13 34 23.5	–58 07 55	sest mar98; sest mar99
13359–6014	13 35 54.6	–60 14 07	sest mar01
13482–6716	13 48 15.4	–67 16 08	sest mar99
13509–6348	13 50 56.8	–63 48 43	sest mar99
13595–5254	13 59 34.4	–52 54 22	sest mar01
14010–5927	14 01 01.7	–59 27 03	sest oct99; sest mar01
14122–5845	14 12 15.2	–58 45 23	sest mar99
14284–5245	14 28 25.5	–52 45 41	sest mar99; sest mar01
14309–5126	14 30 57.3	–51 26 17	sest mar01
14318–6107	14 31 52.5	–61 07 25	sest oct99
14358–6303	14 35 51.2	–63 03 08	sest mar99
14404–6320	14 40 25.1	–63 20 45	sest oct99
14443–5708	14 44 22.0	–57 08 09	sest mar98
14521–6058	14 52 06.1	–60 58 33	sest mar01
15043–5438	15 04 22.2	–54 38 25	sest mar98; sest mar99
15054–5458	15 05 26.9	–54 58 29	sest mar99
15202–5539	15 20 15.9	–55 39 05	sest oct99
15261–5702	15 26 06.3	–57 02 27	sest mar98
15330–5537	15 33 01.6	–55 37 30	sest oct99
15471–5644	15 47 06.3	–56 44 24	sest mar98
15488–4928	15 48 50.2	–49 28 27	sest mar98
16035–5330	16 03 33.6	–53 30 35	sest mar99; sest mar01
16047–5449	16 04 45.6	–54 49 27	sest mar01
16093–4808	16 09 18.8	–48 08 58	sest oct99
16123–4654	16 12 20.2	–46 54 54	sest oct99
16171–4759	16 17 09.5	–47 59 44	sest mar98; sest oct99
16265–5100	16 26 33.5	–51 00 59	sest mar98; sest mar99; sest mar01
16296–4417	16 29 42.0	–44 17 34	sest oct99; sest mar01
16298–5349	16 29 52.2	–53 49 39	sest oct99; sest mar01
16304–3831	16 30 29.3	–38 31 38	sest oct99; sest mar01
16469–4753	16 46 55.3	–47 53 53	sest mar98; sest oct99
16508–4620	16 50 49.0	–46 20 58	sest oct99
16545–4214	16 54 34.3	–42 14 50	sest mar98; sest mar99
16555–4456	16 55 30.5	–44 56 26	sest mar01
16562–5039	16 56 12.3	–50 39 30	sest mar01
17047–2848	17 04 46.4	–28 48 13	sest mar98
17050–4642	17 05 01.7	–46 42 23	sest mar99
17079–6554	17 07 59.4	–65 54 33	sest mar98
17103–3551	17 10 19.6	–35 51 53	sest mar98; sest oct99
17105–3746	17 10 35.8	–37 46 48	sest oct99
17130–3907	17 13 04.8	–39 07 28	sest mar99
17155–4917	17 15 32.8	–49 17 32	sest oct99
17199–3512	17 19 59.5	–35 12 53	sest mar01
17209–3318	17 20 59.8	–33 18 37	sest mar01
17222–2328	17 22 15.8	–23 28 09	iram oct97; sest mar98
17278–3937	17 27 49.5	–39 37 33	sest mar98; sest oct99; sest mar01
17309–3412	17 30 54.8	–34 12 52	sest mar99; sest oct99
17375–3652	17 37 30.4	–36 52 10	sest mar98
17515–2407	17 51 33.2	–24 07 25	iram oct97; sest mar98; sest mar01

Table 1. continued.

Name	RA (1950)	Dec (1950)	Observed
17547-3249	17 54 43.0	-32 49 08	sest mar99
17556+5813	17 55 37.4	58 13 22	iram apr98
17599-4556	17 59 55.8	-45 56 45	sest oct99; sest mar01
18030-1707	18 03 04.6	-17 07 54	iram jul99; sest mar01
18038-1614	18 03 50.9	-16 14 00	sest mar98; sest mar99
18061-2739	18 06 10.0	-27 39 13	iram oct97; sest mar99
18082-2454	18 08 12.9	-24 54 29	sest mar98
18092-0437	18 09 17.5	-04 37 10	iram oct97; iram jul99
18147-2215	18 14 42.0	-22 15 50	sest mar98
18230+0544	18 23 01.8	05 44 18	iram oct97
18234-2206	18 23 27.7	-22 06 07	sest mar98; sest oct99
18244-0108	18 24 27.4	-01 08 03	iram apr98; iram jul99
18276-4717	18 27 37.7	-47 17 48	sest mar98
18289+0420	18 28 54.8	04 20 37	iram apr98; sest mar01
18356-0951	18 35 40.3	-09 51 42	iram oct97; iram apr98; iram jul99
19008+0726	19 00 53.1	07 26 15	iram oct97; sest mar98
19029+2017	19 02 57.4	20 17 26	iram oct97
19108+1155	19 10 53.1	11 55 02	iram oct97; iram apr98
19136+6727	19 13 40.3	67 27 08	iram apr98; iram jul99
19238+1159	19 23 53.6	11 59 03	iram apr98; iram jul99
19248+0658	19 24 48.5	06 58 03	sest mar98
19253+1918	19 25 22.0	19 18 39	iram apr98; iram jul99
19276-0056	19 27 39.8	-00 56 31	iram apr98; sest mar98
19285+1808	19 28 35.7	18 08 48	iram apr98; iram jul99
19289+1931	19 28 56.5	19 31 49	iram apr98; iram jul99
19296+2227	19 29 37.7	22 27 17	iram apr98
19304+2529	19 30 27.0	25 29 41	iram apr98; iram jul99
19358+0917	19 35 49.0	09 17 15	iram apr98; iram jul99; sest mar98
19381+3315	19 38 06.9	33 15 23	iram apr98; iram jul99
19417+3053	19 41 43.4	30 53 09	iram apr98; iram jul99
19419+3222	19 41 56.1	32 22 11	iram jul99
19455+0920	19 45 32.4	09 20 40	iram apr98; iram jul99
19455+2319	19 45 31.2	23 19 06	iram apr98; iram jul99
19457+2346	19 45 42.5	23 46 58	iram apr98; iram jul99
19485+3235	19 48 32.6	32 35 52	iram apr98
19523+2414	19 52 21.9	24 14 25	iram apr98
19524+2130	19 52 25.0	21 30 37	iram apr98
19537+2212	19 53 47.5	22 12 57	iram apr98
19552+3142	19 55 13.7	31 42 17	iram apr98; iram jul99
19558+3333	19 55 53.3	33 33 11	iram apr98
19559+3301	19 55 57.5	33 01 26	iram apr98; iram jul99
20004+2943	20 00 29.1	29 43 14	iram jul99
20014+2830	20 01 24.4	28 30 10	iram apr98
20081+3228	20 08 12.7	32 28 22	iram oct97; iram apr98; iram jul99
20084-1425	20 08 29.3	-14 25 05	sest mar99; sest oct99; sest mar01
20159+3134	20 15 58.9	31 34 50	iram jul99
20171+3519	20 17 06.6	35 19 21	iram oct97; iram apr98; iram jul99
20200+3624	20 20 00.5	36 24 00	iram apr98; iram jul99
20204+2914	20 20 29.1	29 14 01	iram apr98
20253+3814	20 25 22.3	38 14 48	iram apr98; iram jul99
20277+2958	20 27 42.3	29 58 33	iram apr98
20282+3604	20 28 12.2	36 04 31	iram apr98; iram jul99
20323+3153	20 32 22.9	31 53 15	iram apr98; iram jul99
20331+4621	20 33 07.3	46 21 16	iram apr98; iram jul99
20350+5954	20 35 04.0	59 54 56	iram jul99
20351+2618	20 35 10.7	26 18 46	iram jul99; sest mar01
20369+5131	20 36 57.4	51 31 03	iram apr98; iram jul99
20461+4817	20 46 09.1	48 17 49	iram jul99

Table 1. continued.

Name	RA (1950)	Dec (1950)	Observed
20546+6405	20 54 38.1	64 05 48	iram jul99
20564+1857	20 56 29.2	18 57 18	iram jul99; sest oct99; sest mar01
20596+3833	20 59 36.4	38 33 29	iram apr98
21006+4720	21 00 40.1	47 20 12	iram apr98
21027+3704	21 02 42.1	37 04 42	iram apr98; iram jul99
21070+4711	21 07 00.8	47 11 53	iram apr98; iram jul99
21088+4546	21 08 51.7	45 46 28	iram apr98; iram jul99
21160+5546	21 16 05.9	55 46 57	iram jul99
21197-6956	21 19 46.9	-69 56 55	sest mar98
21262+7000	21 26 15.1	70 00 11	iram jul99
21265+5042	21 26 30.7	50 42 17	iram jul99
21324+5537	21 32 24.7	55 37 55	iram apr98
21366+4529	21 36 37.9	45 29 10	iram apr98; iram jul99
21377+5042	21 37 46.9	50 42 49	iram apr98; iram jul99
21383+4513	21 38 18.5	45 13 40	iram apr98
21424+5821	21 42 24.7	58 21 57	iram apr98
21444+5053	21 44 26.8	50 53 33	iram apr98
22039+5328	22 03 57.9	53 28 03	iram jul99
22236+5002	22 23 39.8	50 02 59	iram jul99
23174+6810	23 17 29.9	68 10 14	iram apr98
23234+6434	23 23 29.2	64 34 55	iram apr98
23491+6243	23 49 09.1	62 43 57	iram apr98
23516+6430	23 51 41.8	64 30 48	iram apr98

always found to be within twice the rms values of the last pointing model used by the telescope control software.

The data reduction consisted of several steps. First the individual measurements were reduced. Baselines were removed and all temperatures were put on a main-beam scale (the same applies for all temperatures presented in this paper). The conversion of observed antenna temperature into main-beam temperature requires knowledge of the forward and main beam efficiencies (listed in Table 2 together with the *FWHM* beam widths) and involves a comparison with calibration sources (e.g. Mauersberger et al. 1989 for IRAM). The comparison with the calibration sources (supplemented by consistency checks from stars observed more than once and from published results obtained with IRAM) indicate that the data are consistent. We estimate the final calibration for all observed lines to be accurate to 10% (1σ). Then, the data of the same stars observed during different runs were co-added for IRAM and SEST separately.

The results are outlined in Table 3, available at the CDS, which lists the name of the object, the transition, the channel spacing, the rms noise, the peak temperature, the integrated intensity, the central velocity with respect to the local standard of rest and half the velocity width at zero intensity which equals the expansion velocity of the circumstellar shell. These determined quantities were determined either directly from the profiles or from fits to the profiles made with the reduction program *CLASS*. Typical uncertainties in the central velocity and the expansion velocity are 1 km s^{-1} . The uncertainties in the peak temperature and the integrated intensity are dominated by the calibration uncertainties. Values flagged with a colon are uncertain. Upper limits are 3σ values. The last column contains some

Table 2. The lines observed.

Line	Frequency (MHz)	Teles.	F_{eff}	B_{eff}	<i>FWHM</i> (")
$^{12}\text{CO}(1-0)$	115271.204	IRAM	0.92	0.67	20.9
		SEST		0.70	45
$^{12}\text{CO}(2-1)$	230537.990	IRAM	0.86	0.39	10.4
		SEST		0.60	23
$\text{HCN}(1-0)$	88631.602	IRAM	0.92	0.76	27.0
$\text{SiO}(3-2, v=0)$	130268.702	IRAM	0.90	0.58	18

Note. In July 1999 the beam efficiencies for IRAM were slightly better at 0.71 (CO 1-0), 0.48 (CO 2-1) and 0.77 (HCN).

relevant remarks, for example when the spectrum was severely contaminated by interstellar contamination, or the system temperature when the weather was bad.

The calibrated profiles are shown in the Fig. 1, available in electronic form. Some of the strong interstellar spikes that appear on top of or near the stellar emission profiles and that may be several Kelvin strong have artificially been cut for display purposes. Some panels are intentionally left blank too facilitate comparison of different lines of the same object; the figures are ordered top to bottom, left to right.

4. Results

4.1. General results

The present survey is among the largest conducted for AGB stars in the CO lines and one with the highest detection rate. The largest single survey targeting IRAS objects (AGB stars, PNe, post-AGB, also some YSOs) is that by

Table 3. The observed quantities.

name	transition	Δv km s ⁻¹	rms K	T_{peak} K	$\int T dv$ K km s ⁻¹	V_{LSR} km s ⁻¹	v_e km s ⁻¹	remarks
00422+5310	2-1	1.30	0.016	0.16	2.7	19.4	14.1	
	1-0	1.63	0.04	0.081	1.5	19.4	13.1	
	HCN	1.06	0.011	<0.025	0.4:			
01022+6542	2-1	1.30	0.087					$T_{\text{sys}} = 1400$ K
	HCN	2.11	0.024					
	SiO	2.30	0.022					
01080+5327	2-1	1.30	0.048	0.47	15.0	-20.0	22.6	
	HCN	2.11	0.051	0.15:	4.3			
	SiO	2.60	0.024	0.05:	1.1:			
01443+6417	2-1	1.30	0.061	0.42	16.2	-68.1	30.5	
	1-0	1.63	0.033	0.11:	3.2:	-70:	28:	
	HCN	2.11	0.044	0.08:	3.4:			data corrupted blue wards of -110 km s ⁻¹
02345+5422	SiO	2.30	0.022		0.3:			
	2-1	1.30	0.067	1.22	29.0	-66.0	19.8	
	HCN	2.11	0.070	0.25	5.3			
02596+6639	SiO	2.30	0.024		0.3:			
	2-1	1.30	0.019	0.15	2.7	-41.8	15.8	
	1-0	0.81	0.024	0.048	0.9	-40:		
03157+3258	HCN	1.06	0.010		0.2:			
	2-1	1.30	0.064					iram; $T_{\text{sys}} = 930$ K
	HCN	1.06	0.092					
03238+6034	SiO	2.30	0.026					
	2-1	1.82	0.015	0.10	1.4	-17.5	13.5	sest
	1-0	1.80	0.016	0.09:	1.5	-15.7	17.0:	
	2-1	1.30	0.078	1.06	19.6	-85.5	15.3	
	HCN	2.11	0.073	<0.12	1.2:			
03277+5120	SiO	2.30	0.035	<0.10	0.5:			
	2-1	1.30	0.031	0.11	2.3	-30.2	17.9	
	1-0	0.81	0.047	0.11	2.6	-28.9	16.3	
03293+6038	HCN	2.11	0.007	0.02:	0.3:			
	2-1	1.30	0.081	0.84	22.2	-61.9	21.0	
	HCN	2.11	0.068		2.7:			
03385+5927	SiO	2.30	0.038		0.8:			
	2-1	1.30	0.059	0.32	6.2	-74.5	15.7	
	1-0	1.63	0.031	0.21	4.8	-74.9	17.2	
03557+4404	HCN	2.11	0.063		0.8:			
	SiO	2.30	0.021					
	2-1	1.30	0.039	0.36	6.0	-49.2	14.7	
04127+5030	1-0	1.63	0.031	0.39	6.8	-47.6	15.0	
	HCN	2.11	0.017	0.05:	0.8:			
	SiO	2.30	0.018		0.2:			
04179+5951	2-1	1.30	0.022	0.23	6.5	-0.1	17.9	
	1-0	1.63	0.016	0.066	1.4:	-0.2:	16.8:	
	HCN	2.11	0.008	0.048	1.1:	1.3	17.1	
04297+2941	2-1	1.30	0.055	0.65	20.3	4.2	23.4	
	1-0	1.63	0.033	0.28	9.4	4.4	22.5	
	HCN	2.11	0.017	0.09	2.6	6.9	19.6	
04365+6349	SiO	2.30	0.024		0.6:			
	2-1	1.30	0.045	<0.12	1.6:			iram; $T_{\text{sys}} = 1450$ K
	1-0	1.63	0.018	0.11	2.5	3.5	17.7	
04365+6349	HCN	2.11	0.011	0.048	1.1	5.4	17.2	
	2-1	1.82	0.018					sest; interstellar contamination
	1-0	1.80	0.019	0.05:				
04365+6349	2-1	1.30	0.124	0.43	7.1	-47.0	14.2	$T_{\text{sys}} = 1870$ K
	HCN	1.06	0.045	0.1:	1.7:			
	SiO	2.30	0.025		0.5:			

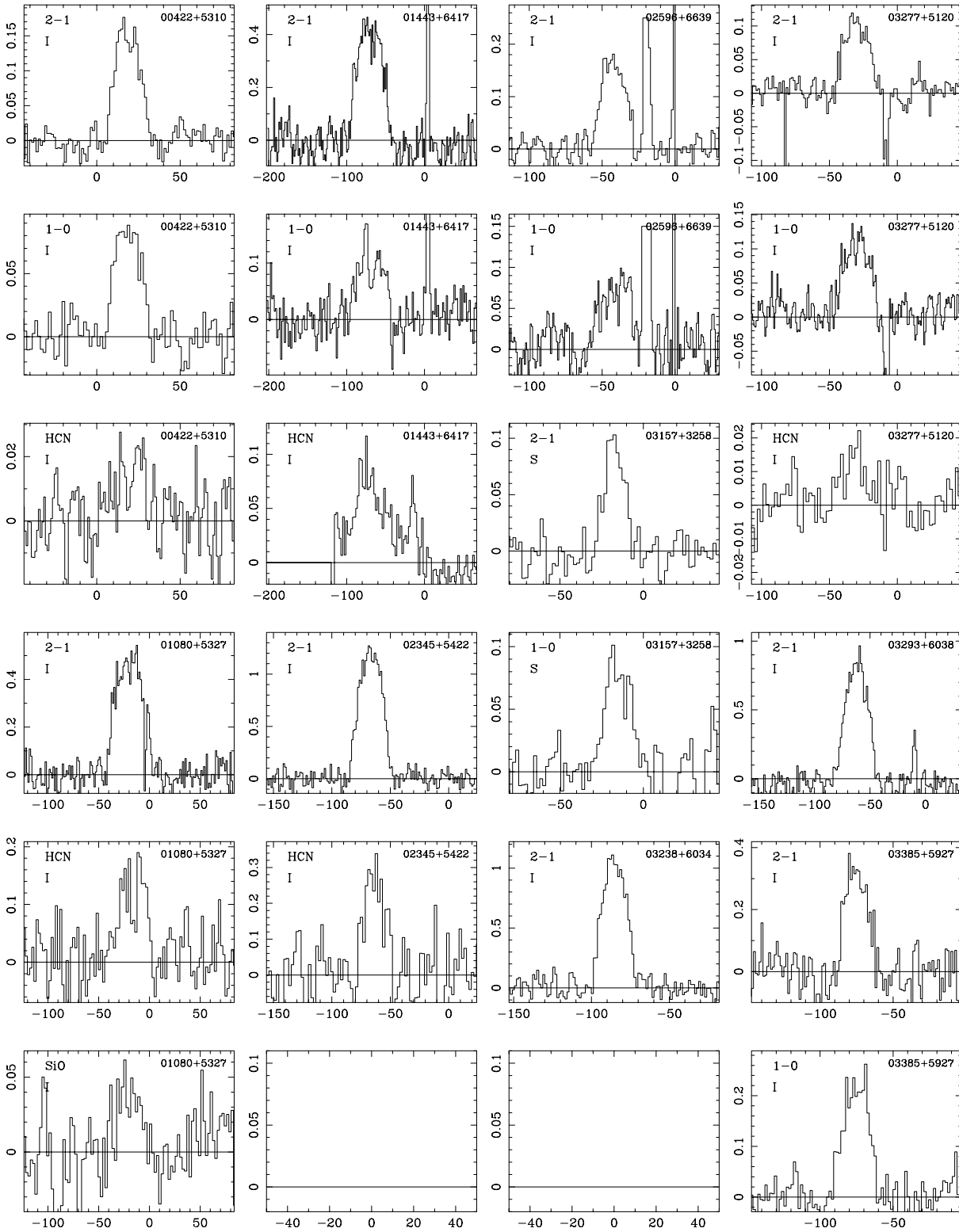


Fig. 1. Plotted are the velocity w.r.t. the LSR, and the main-beam temperature in Kelvin. The figures are ordered top to bottom, left to right. Some panels are intentionally left blank in order to always have the observations of the same stars below each other so that the velocity scales are lined up for easy comparison.

Nyman et al. (1992), who observed 519 objects in the CO (1–0) line with SEST and detected 163 objects. Compared to their survey the present one uses more sensitive receivers and has the benefit of also observing CO (2–1) that is usually the stronger

line. The present survey is probably the second largest aiming at AGB stars, and the largest specifically targeting carbon stars. A smaller survey, concentrating on carbon stars in the Galactic plane, is that by Kastner et al. (1993) who detected 47 out of

58 stars observed in CO (1–0) and (2–1) with IRAM. Olofsson et al. (1993) detected 68 out of 99 observed bright ($K < 2$ mag) optically identified carbon stars with OSO, IRAM and SEST in CO (1–0) and (2–1). Kerschbaum et al. (1999) observed 109 O-rich SR and Irregular variables in several CO lines with several telescopes, detecting 66. Numerous smaller surveys in CO, or mapping observations of previously CO detected objects, or surveys aimed at obtaining molecular abundances in previously CO detected objects exist.

In the end, all 252 stars on the observing list were observed. Of the 96 stars observed only with IRAM, 86 were detected in at least one line. Five of the non-detections may be inhibited by strong interstellar contamination. Of the 134 stars observed only with SEST, 101 were detected in at least one line, with 31 non-detections possibly inhibited by strong interstellar contamination. Twenty-one stars were observed with both telescopes, with 10 detected by IRAM and 13 by SEST in at least one line. Many of these sources observed with SEST had been observed with IRAM first (because of the expected higher sensitivity) under adverse weather conditions (the system temperatures have been listed in the ‘remarks’ column to mark these objects as candidates to be re-observed with IRAM under improved weather conditions). Overall 80% of the observed sources have been detected in at least one line. Many of the non-detections are sources in the Galactic plane observed with SEST which is less sensitive than IRAM to point sources and picks up more interstellar emission in its larger beam.

4.2. Comparison of IRAM and SEST observations

Since in almost all cases the SEST observations were only performed because the IRAM observations had been made under adverse weather conditions, or to obtain CO (1–0) data when the IRAM 1.3 mm receiver had been tuned to HCN, only five stars have good data obtained with both telescopes. In these cases the ratio of the CO (1–0) and/or CO (2–1) integrated intensities between IRAM and SEST is between 3.2 and 4, what is approximately the expected ratio given the respective beam sizes.

4.3. SiO and HCN data

Of the 68 objects also observed in the SiO line, only one was convincingly detected (IRAS 19008+0726) and two marginally (IRAS 01080+5327, 20596+3833). These three are all optically identified carbon stars, being respectively number 4162, 180, and 5089, in the General Catalog of Cool Carbon stars (GCCCS, Stephenson 1989). Their carbon star nature is beyond any doubt.

The presence of oxygen-rich molecules in the envelopes around carbon stars is well documented (Bujarrabal et al. 1994; Olofsson et al. 1989; Biegging et al. 2000 and references therein) and integrated intensities or line-ratios between two species are usually used to discriminate between O- and C-rich sources. Bujarrabal et al. (1994) quote a lower limit of 2.8 for O-rich and an upper limit of 0.33 for C-rich sources for the SiO (3–2)/HCN (1–0) ratio of the integrated intensities.

In the three stars just mentioned the ratio of the line intensities is $1.1/4.3 = 0.26$, $9.4/66.0 = 0.14$ and $1.1/1.5 = 0.73$ in IRAS 01080+5327, 19008+0726, 20596+3833, respectively. In the last case, both HCN and SiO integrated intensities are uncertain, and for the first two cases the ratio is in agreement with the upper limit derived by Bujarrabal et al. (1994).

The ratio HCN (1–0)/CO (1–0) is known to be as low as 0.17 in C-rich objects (Olofsson et al. 1998) and none of the twenty-four objects with reliable detections in both lines have an integrated intensity ratio lower than this.

In summary, the observations of the SiO and HCN lines give results that are in agreement with the line ratios expected for carbon stars.

Acknowledgements. This program was initiated, and part of the observations were obtained, when MG was a research fellow at the Max-Planck Institut für Astrophysik, Garching, Germany. We would like to thank the program committees of ESO and IRAM for their continuing support. This research has made use of the SIMBAD database, operated at CDS, Strasbourg, France. René Oudmaijer is thanked for commenting upon an earlier version of the manuscript.

References

- Aaronson, M., Blanco, V. M., Cook, K. H., & Schechter, P. L. 1989, *ApJS*, 70, 637
- Aaronson, M., Blanco, V. M., Cook, K. H., Olszewski, E. W., & Schechter, P. L. 1990, *ApJS*, 73, 841
- Biegging, J. H., Shaked, S., & Gensheimer, P. D. 2000, *ApJ*, 543, 897
- Bujarrabal, V., Fuente, A., & Omont, A. 1994, *ApJ*, 421, L47
- Dejonghe, H. 1989, *ApJ*, 343, 113
- Durand, S., Dejonghe, H., & Acker, A. 1996, *A&A*, 310, 97
- Groenewegen, M. A. T., de Jong, T., van der Blik, N. S., Slijkhuizen, S., & Willems, F. J. 1992, *A&A*, 253, 150
- Groenewegen, M. A. T., Baas, F., de Jong, T., & Loup, C. 1996, *A&A*, 306, 241
- Groenewegen, M. A. T., Van den Hoek, L. B., & de Jong, T. 1995, *A&A*, 293, 381
- Josselin, E., Loup, C., Omont, A., et al. 1998, *A&AS*, 129, 45
- Kastner, J. H., Forveille, T., Zuckerman, B., & Omont, A. 1993, *A&A*, 275, 163
- Kerschbaum, F., & Olofsson, H. 1999, *A&AS*, 122, 167
- Knapp, G. R., Young, K., Lee, E., & Jorissen, A. 1998, *ApJS*, 117, 209
- Loup, C., Forveille, T., Omont, A., & Paul, J. F. 1993, *A&AS*, 99, 291
- Mauersberger, R., Guélin, M., Martin-Pintado, J., et al. 1989, *A&AS*, 79, 217
- Neri, R., Kahane, C., Lucas, R., Bujarrabal, V., & Loup, C. 1998, *A&AS*, 130, 1
- Nyman, L.-A., Booth, R. S., Carlström, U., et al. 1992, *A&AS*, 93, 121
- Olofsson, H., Eriksson, K., Gustafsson, B., & Carlström, U. 1993, *ApJS*, 87, 267
- Sevenster, M. N., Dejonghe, H., & Habing, H. J. 1995, *A&A*, 299, 689
- Sevenster, M. N., Dejonghe, H., Van Caelenberg, K., & Habing, H. J. 2000, *A&A*, 355, 537
- Stephenson, C. B. 1989, *Publ. Warner & Swasey Obs.*, 3
- Volk, K., & Cohen, M. 1989, *AJ*, 98, 931
- Volk, K., Kwok, S., & Langill, P. P. 1992, *ApJ*, 391, 285
- Volk, K., Kwok, S., Stencel, R. E., & Brugel, E. 1991, *ApJS*, 77, 607